
FlashOverlap: A LIGHTWEIGHT DESIGN FOR EFFICIENTLY OVERLAPPING COMMUNICATION AND COMPUTATION

Ke Hong^{1,2} Xiuhong Li² ✉ Minxu Liu² Qiuli Mao² Tianqi Wu^{1,2} Zixiao Huang^{1,2}

Lufang Chen² Zhong Wang² Yichong Zhang¹ Zhenhua Zhu¹ Guohao Dai^{2,3} ✉ Yu Wang¹ ✉

✉ lixiuhong@infini-ai.com, daiguohao@sjtu.edu.cn, yu-wang@tsinghua.edu.cn

ABSTRACT

Generative models have achieved remarkable success across various applications, driving the demand for multi-GPU computing. Inter-GPU communication becomes a bottleneck in multi-GPU computing systems, particularly on consumer-grade GPUs. By exploiting concurrent hardware execution, overlapping computation and communication latency is an effective technique for mitigating the communication overhead. We identify that an efficient and adaptable overlapping design should satisfy (1) tile-wise overlapping to maximize the overlapping opportunity, (2) interference-free computation to maintain the original computational performance, and (3) communication agnosticism to reduce the development burden against varying communication primitives. Nevertheless, current designs fail to simultaneously optimize for all of those features.

To address the issue, we propose *FlashOverlap*, a lightweight design characterized by tile-wise overlapping, interference-free computation, and communication agnosticism. *FlashOverlap* utilizes a novel signaling mechanism to identify tile-wise data dependency without interrupting the computation process, and reorders data to contiguous addresses, enabling communication by simply calling NCCL [1] APIs. Experiments show that such a lightweight design achieves up to $1.65\times$ speedup, outperforming existing works in most cases.

1 Introduction

In recent years, generative models have revolutionized various fields, powering applications including chatbots [2, 3, 4], code assistants [5, 6], video generation [7, 8, 9, 10], and agent systems [11, 12]. To continuously enhance the intelligence capabilities of generative models, the number of parameters has dramatically increased, *e.g.*, DeepSeek-V3 [2] contains 671B parameters. Meta has recently previewed its most powerful model, Llama 4 Behemoth [13], which scales to 2T parameters. The computing devices, such as GPUs, typically offer limited memory capacity, making it infeasible to accommodate those massive parameters on a single GPU for generative model deployment. Consequently, parameter partitioning across multiple devices has become essential, typically through tensor parallelism (TP), pipeline parallelism (PP), and expert parallelism (EP). Such a multi-GPU computing paradigm inevitably introduces non-negligible inter-GPU communication overheads, primarily arising from collective communication operations such as AllReduce, ReduceScatter, and All-to-All. To achieve cost efficiency, large language model (LLM) inference prefers consumer-grade GPUs (*e.g.*, NVIDIA 4090, L20) for deployment. However, deployment on consumer-grade GPUs aggravates the communication overhead, as PCIe interconnection (typically offering 16-64 GB/s bidirectional bandwidth) serves as the primary communication channel between devices.

¹ Tsinghua University

² Infinigence-AI

³ Shanghai Jiao Tong University

✉ Corresponding authors: Yu Wang, Xiuhong Li, Guohao Dai.

Table 1: Comparison of *FlashOverlap* and existing works.

Method	Tile-wise Overlapping	Interference-free Computation	Communication Agnostic
Decomposition-based [15, 16, 17, 18, 19, 20]	×	×	✓
Fusion-based [21, 22, 23, 24, 25, 26]	✓	×	×
Signaling-based (ours)	✓	✓	✓

Overlapping computation and communication has emerged as an effective technique to mitigate communication overhead. The core idea lies in executing computation with communication operations asynchronously, to fully exploit the heterogeneous hardware. In generative models, the computation part is typically general matrix multiplication (GEMM), and is executed on the high-throughput Tensor Core, while the communication part utilizes specialized inter-connection hardware such as NVLink [14]. Unfortunately, data dependency between computation and communication prevents the concurrent execution. To resolve the data dependency, two mainstream methods have been proposed. (1) Decomposition-based method decomposes the output tensor of the computation operation into multiple subtensors, enabling asynchronous overlap between communication for the k -th subtensor and computation for the $(k + 1)$ -th subtensor. (2) Fusion-based method that fuses computation operators with communication operators into a single GPU kernel, exploiting inter-tile computation and communication overlap through fine-grained scheduling, where a tile is the minimum independently paralleled data unit on the GPU.

To ensure data contiguity, the decomposition-based method is constrained in the tensor decomposition patterns, resulting in misalignment with modern GPU parallel computing paradigms, and consequently fails to exploit tile-wise fine-grained overlapping. Besides, if the scale is insufficient, the fragmented computation will fail to fully utilize the GPU computational resources, thereby negating the performance benefits of overlap. The fusion-based method requires prohibitive manual optimization requirements. On one hand, fusion requires manually implemented communication primitives, failing to utilize the existing high-performance communication library such as NCCL [1]. Consequently, this method suffers from low generalizability - each communication primitive (AllReduce, ReduceScatter, etc.) demands a customized fusion implementation. On the other hand, aligning the data granularity between computation and communication may require modifications to the computational logic or tiling strategies, potentially preventing the computation from achieving optimal performance.

In this paper, we identify that an efficient and adaptable overlapping design should satisfy (1) tile-wise overlapping to maximize the overlapping opportunity, (2) interference-free computation to maintain the original computational performance, and (3) communication agnosticism to reduce the development burden against varying communication primitives (AllReduce, ReduceScatter, All-to-All, etc.). We categorize the existing works in Table 1, and propose a novel signaling-based overlapping design named *FlashOverlap*. The core idea of *FlashOverlap* is a signaling mechanism that triggers communication without interrupting the primary logic of computation. Moreover, *FlashOverlap* has no requirements on the specific implementation of communication primitives, triggering communication by direct NCCL [1] calls.

Based on the signaling mechanism, we observe the inherent "wave" pattern on top of tiles in GEMMs, and construct independent computation and communication data dependencies based on waves. Specifically, *FlashOverlap* triggers communication of the corresponding tiles through signaling after the finished computation of several waves (denoted as a wave group). Then, to ensure communication continuity, *FlashOverlap* introduces a pre-communication reordering operation to write data to contiguous addresses for communication, then conducts the post-communication reordering in subsequent operators (e.g., RMSNorm) to correct the order. Moreover, the selection of each wave group size constitutes a design space, and we propose a predictive search based on prediction models for rapid solving of the solution.

In summary, this paper makes the following contributions:

- We introduce a novel signaling-based design, *FlashOverlap*, to achieve computation-communication overlap, characterized by tile-wise overlapping, interference-free computation, and communication agnosticism.
- Based on the signaling mechanism, we demonstrate that the tile-wise signaling can be resolved into waves to mitigate communication fragmentation. Besides, we employ a pair of pre-communication and post-communication reordering operations to ensure communication continuity, and the overhead of both is optimized via kernel fusion.

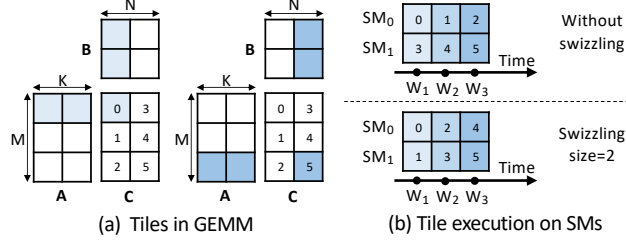


Figure 1: Tile partition and execution in GEMM.

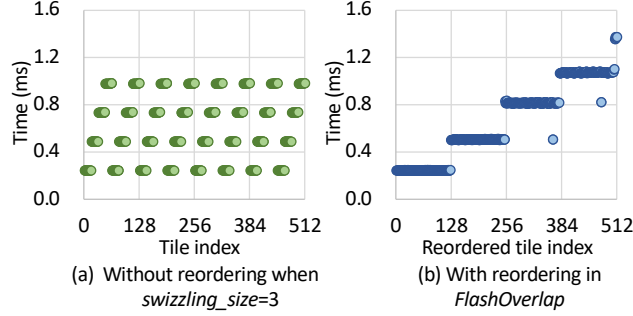


Figure 2: Wave pattern in GEMM execution. Each point in (a) and (b) represents the corresponding completion time of each tile, and the time is captured by the global timer [27].

- We enable the design of *FlashOverlap* to be tunable via wave grouping, and propose a predictive search method to optimize the wave group size selection.
- We conduct experiments to evaluate *FlashOverlap*, the results demonstrate that *FlashOverlap* delivers 69-98% of the theoretical performance and achieves up to $1.65\times$ speedup through computation-communication overlap.

2 Background

In this section, we elaborate on the characteristics of the GEMM computation and the existing inter-GPU communication implementations on modern GPUs. Subsequently, we demonstrate that GEMM computation followed by data-dependent communication can be commonly found in both training and inference of generative models, where the communication leads to a significant portion of latency, emerging as one of the primary bottlenecks for improving efficiency in multi-GPU computing systems. Based on that, we present a comprehensive survey and comparative analysis of prior works for computation-communication overlap.

2.1 General Matrix Multiplication

2.1.1 Wave Pattern in GEMM

As the core component in neural networks, general matrix multiplication (GEMM) can be formulated as $A^{M \times K} \times B^{K \times N} = C^{M \times N}$, where M, N, K collaboratively represent the GEMM size. Modern GPUs consist of multiple streaming multiprocessors (SMs) [28], where each SM contains independent computational and on-chip memory resources. To exploit the parallel execution across SMs, a GEMM workload is partitioned into tiles distributed across SMs. As depicted in Fig. 1, the output matrix C is partitioned into tiles, with each tile’s workload including the corresponding data loading and computation from the input matrices A and B . Those tiles are scheduled across different SMs for parallel execution, and the scheduling order is influenced by techniques such as block swizzling [29]. A concrete example is illustrated in Fig. 1, where six tiles are distributed across two SMs. Consequently, the tile execution follows a specific sequential order. Notably, the completion time of the tiles exhibits a distinct wave pattern.

A wave is defined as a set of concurrently executed tiles [30]. As shown in Fig. 2, we capture the completion time of each tile in a GEMM ($M = 2048, N = K = 8192$) on an RTX 4090 GPU, and the tile completion time can be distinctly categorized into four distinct waves, which is consistent with the result of dividing tile number (512) by SM number (128). Furthermore, we observe that the completion order of tiles does not align with the memory address

(represented by tile index). Such address discontinuity prevents early-finished tiles from being promptly communicated. To address the mismatch and enable efficient computation-communication overlap, *FlashOverlap* performs a reordering among tiles, which is detailed in Sec. 3.3.

2.1.2 Main Loop and Epilogue

The implementation of GEMM involves the main loop and the epilogue. The main loop performs the core multiply-accumulate operations and accounts for the majority of the GEMM duration, while the epilogue refers to element-wise operations (*e.g.*, ReLU, SiLU, or bias addition) performed after matrix multiplication. Those element-wise operations can typically be fused with the preceding matrix multiplication into a single GPU kernel [31], thereby eliminating redundant memory accesses and kernel launch overhead.

2.2 Inter-GPU Communication

The underlying behaviours of inter-GPU communication vary significantly across different hardware configurations (intra-node or inter-node, via NVLink [14], PCIe [32], or InfiniBand [33], etc.). Aimed at hiding the interconnect hardware complexities from users, libraries such as the NVIDIA collective communications library (NCCL) [1] provide high-level APIs for various communication primitives. NCCL supports encapsulated collective communication primitives including AllReduce, AllGather, and ReduceScatter, as well as point-to-point send/receive operations, which can be used for constructing the All-to-All primitive. Besides the convenience, NCCL also optimizes efficiency for communication, such as implementing the RING algorithm [34] for better bandwidth efficiency. The communication-agnostic design enables *FlashOverlap* to leverage NCCL’s communication capabilities through standard API calls directly. Note that other libraries such as MSCCLang [35] and DeepEP [19] are achieving similar functionality, and can also be seamlessly integrated into *FlashOverlap* through API calls.

2.3 Computation Followed by Data-Dependent Communication

In multi-GPU computing systems, each GPU is responsible for only part of the overall computation, thereby necessitating communication for data exchange and synchronization. Such a pattern is highly prevalent, as illustrated in the following cases:

- **GEMM+AllReduce:** Applying parallelism methods to model inference or training frequently triggers an AllReduce primitive after a GEMM. Specifically, the tensor parallelism (TP) needs an AllReduce operation to reduce the GEMM partial results from all the GPUs in the parallel group [36], and the data parallelism (DP) uses an AllReduce operation to compute gradient summation across all GPUs [37]. GEMM+AllReduce is widely utilized in multi-GPU computing, but it incurs significant communication overhead due to the high complexity of the AllReduce primitive.
- **GEMM+ReduceScatter:** In model training with TP, AllReduce is typically decomposed into a ReduceScatter and an AllGather, and the ReduceScatter and its preceding GEMM form a GEMM+ReduceScatter pattern. Besides, the backward pass of fully shared data parallelism (FSDP) performs ReduceScatter on weight gradients after GEMM computation [38].
- **GEMM+All-to-All:** The widely adopted Mixture-of-Experts (MoE) models [39] typically employ expert parallelism (EP) to distribute experts across multiple GPUs. In this paradigm, as data is dynamically routed to specific experts on particular GPUs, an All-to-All communication operation is necessary to transfer the processed data back to the original GPUs after expert computation. Specifically, the MoE part contains linear layers, which leads to the GEMM+All-to-All pattern. Notably, the dynamic routing mechanism creates inherent workload imbalance among GPUs, exacerbating the existing communication overhead.

2.4 Related Works

Prior research has extensively investigated the overlapping technique to mitigate communication bottlenecks in multi-GPU computing systems. Regarding overlapping techniques, existing works can broadly be classified into two categories: (1) overlapping data-dependent computation and communication, and (2) leveraging existing multiple dataflows to enable overlap. For the first category concerning data-dependent computation and communication, tensor decomposition and kernel fusion are the predominant approaches.

Table 2: Notation description.

Notation	Description
M	Input dimension in a GEMM
N	Output dimension in a GEMM
K	Accumulation dimension in a GEMM
T	Number of waves
P	Number of groups
W_i	The i -th wave
G_j	The j -th group

2.4.1 Decomposition-based Method

CoCoNet [15] demonstrates the importance of scheduling computation order to align with the communication order, and further designs a compiler-based approach to automatically generate efficient GPU kernels that coordinate computation and communication. [17] also utilizes a compiler-based approach, introducing a cost model to handle the trade-offs between overlap opportunity and degradation brought by segmentation. Domino [16], Async-TP [40], and MegaScale [20] have applied the decomposition-based method to LLM training in practice. Centauri [18] builds a comprehensive communication partition space and performs hierarchical scheduling to maximize overlapping efficiency in large language model (LLM) training. While careful optimization of decomposition strategies (*e.g.*, decomposition granularity and dimension) enhance performance, decomposition-based methods fundamentally cannot achieve tile-wise overlapping, and hence the potential improvement remains limited.

2.4.2 Fusion-based Method

In [22], the AMD team designs the fusion paradigms of embedding+All-to-All, general matrix-vector multiplication (GEMV)+AllReduce, and GEMM+All-to-All on AMD GPUs. FLUX [21] optimizes for TP, fusing the communication into the beginning or end of the highly optimized GEMM kernel at the tile level, by sharing the address used in remote access. Comet [23] introduces a thread block specialized kernel to implement GEMM+All-to-All for MoE layers, distributing computation and communication to different SMs for parallel execution, where the SM ratio between the two operations can be adjusted for better efficiency. To reduce the development effort, TileLink [26] introduces a compiler-based approach to automatically generate the overlapping GPU kernel using tile-centric primitives. NVIDIA also develops cuBLASMP [25] to support such fusion. Although implementation details differ, fusion-based methods universally adopt tile-wise overlapping to achieve improved overlapping efficiency. However, kernel fusion creates new demands for communication implementation and optimization, and necessitates additional synchronization logic when coordinating computation and communication pipelines. Besides, T3 [41] explores fine-grained fusion under non-invasive GEMM modifications, tracking the progress of tiles to trigger communication. However, T3 relies on a specific hardware design and is evaluated in simulation, which still faces challenges in real multi-GPU systems.

2.4.3 Multi-dataflow Scheduling

Another line of research [42, 2, 43, 44] exploits multi-dataflow scheduling to achieve overlap. Those works exploit inherent parallel data dependencies (*i.e.*, multi-dataflows), including those between forward and backward passes, among MoE experts, and between weight and activation gradients during backpropagation, to achieve computation and communication overlap across different dataflows. Although multi-dataflow scheduling demonstrates promising results, its applicability remains constrained to specific scenarios, and hence is not the main focus of this work.

3 Lightweight Overlapping Design

3.1 Overview

The overview of *FlashOverlap* is illustrated in Fig. 3, and the GEMM computation remains a single GPU kernel with the proposed overlapping design, sending signals to trigger communication. Considering data dependency, the signal ensures that the communicated tiles finish the corresponding GEMM computation. Moreover, *FlashOverlap* performs pre-communication and post-communication reordering operations to create contiguous addresses for communication.

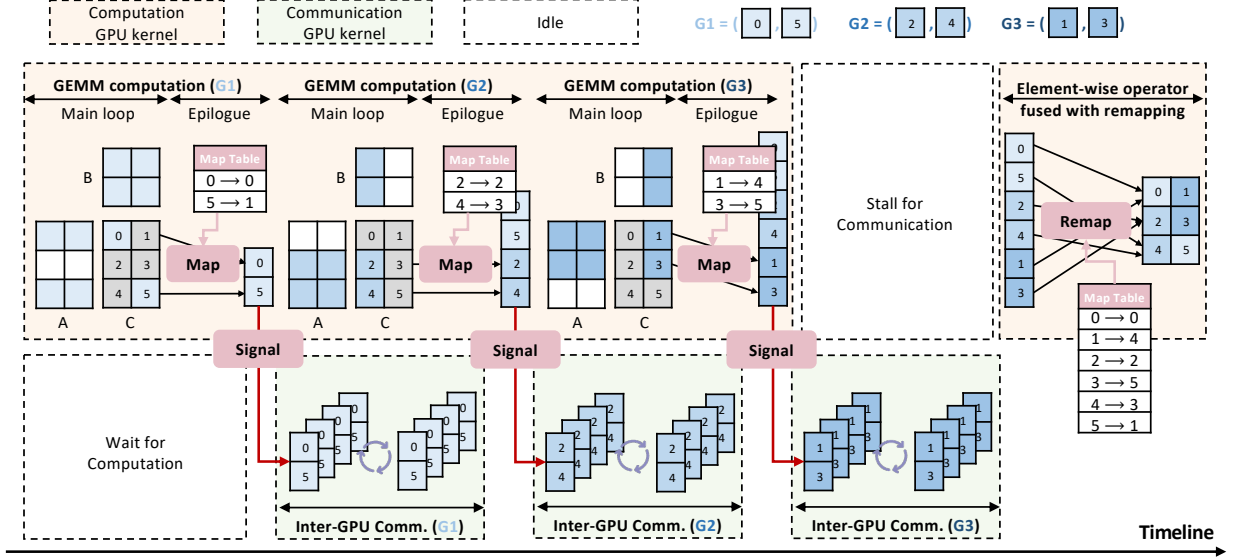


Figure 3: Overview of *FlashOverlap*. The GEMM computation is executed within one GPU kernel, and when each group (G_1 , G_2 , or G_3) finishes, it first reorders the tiles in the group to contiguous addresses, and then signals to trigger the corresponding inter-GPU communication of the group. To correct the order, *FlashOverlap* reorders the tiles back when communication finishes.

3.2 Signaling

3.2.1 Motivation: Data Dependency.

A signaling mechanism is necessary to track the fully computed data that is ready for communication without interrupting the GEMM computation. In decomposition-based works [15, 16, 17, 18, 19, 20], the communication is directly triggered upon completion of the decomposed GEMM computation. Fusion-based implementations [21, 22, 23, 24, 25, 26] employ instruction scheduling to chain the dependent computation and communication operations. However, both strategies require modifications to the native GEMM computation pipeline. To avoid such interruption, ideally, when a certain part of the data finishes GEMM computation, a signal can be used to initiate the corresponding communication while the GEMM kernel continues the computation.

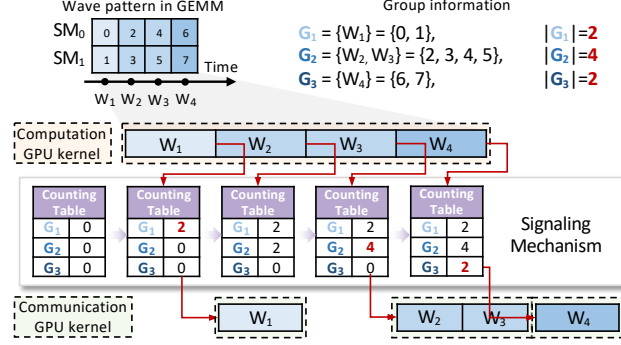
3.2.2 Challenge: Signaling Granularity.

To build such a mechanism, we ought to determine the signaling granularity, and directly applying the tile-wise signaling is not enough. Since coarse-grained signals can hinder effective computation-communication overlap, previous fusion-based works [21, 23, 26] suggest that tile-wise granularity is effective for implementing fine-grained data dependencies between the GEMM computation and the communication, as a tile is the minimal parallel data unit in GEMM. However, directly applying tile-wise signaling leads to significant communication fragmentation. Therefore, the proposed mechanism necessitates further optimization of the signaling granularity. In addition, tunable granularity is desirable for adaptability to workload.

3.2.3 Insight: from Tile to Wave, from Wave to Group.

Instead of signaling for a tile, *FlashOverlap* signals for a group of tiles together. We first investigate the GEMM computation and exploit the wave-like execution pattern. The wave pattern in Fig. 2 denotes that certain tiles (*i.e.*, a wave) are completed nearly simultaneously, typically within 5% of the wave duration. Therefore, the tile-wise signaling is not necessary, and we can directly use a wave of tiles for signal bundling to trigger the communication, which delivers essentially the same overlap opportunity.

However, static wave-wise signaling is not optimal against workload variety. A trade-off exists between smaller but immediate communication and larger but delayed communication. To achieve the tunable granularity, we further define the group on top of the waves. A group G includes $|G| \geq 1$ waves, and the corresponding communication starts after each group finishes the GEMM computation. The size of a group is a tunable configuration.

Figure 4: Signaling mechanism in *FlashOverlap*.

3.2.4 Approach: Group-wise Tile Counting.

We introduce a tile-counting table to track the GEMM computation process, and the finished tiles are recorded separately by groups. Specifically, the counting table is of size P , indicating the tiles are divided into P different groups (G_1, G_2, \dots, G_P). The i -th number in the counter is atomically added by 1 when a tile in $G_i, i \leq P$ is finished. Once the i -th number reaches $|G_i|$, the communication of G_i starts. *FlashOverlap* uses the tile index to identify which group a tile belongs to.

As shown in Fig. 4, there are 3 groups (G_1, G_2, G_3), with each including tiles of 1 or 2 waves. The counting table is initialized to all zeros. When the first wave W_1 finishes, tile 0 and tile 1 are recorded for G_1 in the table. The counting number reaches $G_1 = 2$, thereby triggering the communication of the tiles in G_1 (also W_1). For G_2 with 2 waves (4 tiles), the communication holds until the counting number reaches 4, and all four tiles are communicated together. The behavior of G_3 is the same as that of G_1 .

3.3 Reordering

3.3.1 Motivation: Contiguous Addresses for Communication.

Contiguous addresses are essential for avoiding bandwidth utilization degradation. A single inter-GPU communication behavior (e.g., calling NCCL [1] library) necessitates contiguous addresses for both the sending and receiving buffers. Incontiguous addresses force multiple communication calls, which leads to segmented communications and under-utilized bandwidth. We capture the bandwidth curve varying with the data amount on RTX 4090 and A100 GPUs, and discover a sharp degradation when the data amount falls below a certain threshold, as shown in Fig. 8. Therefore, large and contiguous data blocks are desirable for inter-GPU communication.

3.3.2 Challenge: Irregular Tile Execution Order.

Unfortunately, the tile execution order tends to be irregular in GEMMs, which leads to only small and incontiguous data blocks being ready for communication before the GEMM computation finishes. The underlying reason for such irregularity is the application of block swizzling [29], which is an optimized technique for GEMM performance. Block swizzling schedules the data tile onto GPU blocks in a swizzling manner for enhanced memory access efficiency. Fig. 5 (a) and (b) show a typical tile execution order with swizzling size = 2. After the first wave W_1 (also the first group G_1 in the figure), the finished tile 0 and tile 3 are not contiguous in addresses.

3.3.3 Insight: Data Order Can be Incorrect.

The correct data order is not strictly required for inter-GPU communication, which allows us to reorder those incontiguous tiles to form a large and contiguous data block. (1) AllReduce: the requirement is to maintain consistent tile order across all GPUs, while this tile order can be entirely different from that in the original GEMM output matrix without affecting the correctness of communication. (2) ReduceScatter: the rows are sliced onto different GPUs. Therefore, the tile order should be carefully managed to ensure that every complete row is sent to a certain GPU, while which row to which GPU does not inherently matter. (3) All-to-All primitive: the data division across different GPUs is at the token level, and a row is specifically dedicated to a determined GPU. To conclude, although communication primitives bring some limitations on the data order to ensure communication correctness, there is space remaining for reordering.

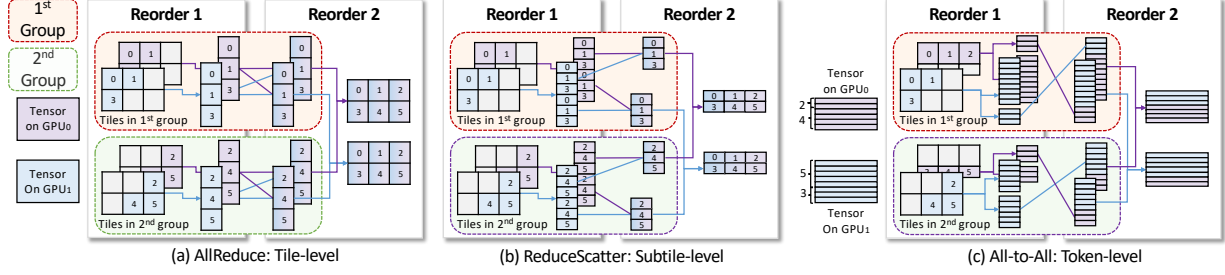


Figure 5: Reordering patterns under different primitives.

3.3.4 Approach: Execution-Order-Aware Reordering

For the AllReduce primitive, *FlashOverlap* reorders the tiles to contiguous addresses according to their execution order. Note that the tile order within the same wave can be random, but the inter-wave order influences the overlapping efficiency. Therefore, we establish the tile-to-wave relationship based on the GEMM parameters (e.g., tiling size and sizzling pattern) and generate the mapping table to record the tile mappings. Specifically, the map table's key records the original tile index, and the corresponding value records the reordered tile index. Assuming W_i is the index set of the tiles belonging to the i -th wave, first W_i is sorted ascendingly to be W'_i . The original tile index $x = W'_i[j]$, and the reordered tile index $y = i \times \text{wave_size} + j$.

As mentioned in Sec. 3.3.3, the other two primitives necessitate more careful design. For the ReduceScatter primitive, each tile is split equally by the rows to form subtiles as many as GPU number. Instead of a tile, a subtile is utilized as the reordering unit. In this way, no matter how the tiles are assigned to GPUs, the k -th subtile in the tile always resides on the k -th GPU at the end, so as the row satisfying $\text{row_id} \% \text{gpu_number} = k$. For the All-to-All primitive, we introduce a specific memory pool for each destination GPU to exclusively store the data sliced by tokens. Specifically, when a group finishes computation and sends the signal, we perform corresponding communication for the data in all of the memory pools.

3.3.5 Approach: Reordering based on Kernel Fusion

The pre-communication reordering process is fused into the GEMM computation, involving only the epilogue without interrupting the main loop. Since the mapping table's size is negligible compared to the matrix, it brings nearly no extra memory access.

After the communication, we need a reordering operation to restore the original data order, which can be seamlessly fused into the subsequent element-wise kernel. As illustrated in Fig. 6, instead of directly loading data (tile, subtile, or token) based on the original index (left white part), the fused kernel loads data based on the mapped index (right red part). Although the access pattern is changed, the memory efficiency is well preserved due to the guaranteed locality of sufficiently contiguous data. We provide a comprehensive quantitative analysis of the associated overhead in Sec. 6.5.

3.4 Design Space

FlashOverlap is characterized by the tunable configuration for grouping to optimize the overlapping performance. We formulate a binary discrete decision optimization problem, and the optimization objective is to minimize the latency with overlapping. After each wave, the tiles can be decided to be communicated (denoted as "1") or not (denoted as "0"). The last wave is the exception, as all the accumulated tiles must be communicated. Assuming there are T waves, the design space is of size 2^{T-1} . Consider the first example in Fig. 7, we choose to conduct communication after W_1 , W_3 and W_5 , thus deriving the wave partition of (1, 2, 2). The group sizes are $|G_1| = 1$, $|G_2| = 2$, $|G_3| = 2$, respectively. In the second example, the communication is triggered after W_2 and W_5 , with the wave partition being (2, 3). Such a partition leads to two groups with sizes of 2 and 3, respectively.

Note that the design space is much more compact than that of the existing fusion-based method. As discussed in Sec. 1, due to significant modifications to the GEMM computation, the kernel fusion method requires co-optimization of computational and communication operations. Although there are already compiling works addressing the overhead issue [26], making the tuning process automatic, the design space includes the separate optimization for the GEMM and the communication primitive, and the co-design of the linking efficiency.


```

void elt_kernel (T *input, T *output,
                int tile_idx){
    T data[...];

    load_tile(data, input[tile_idx]);
    output[tile_idx] = element_wise_op(data);
}

void elt_remap_kernel (T *input, T *output,
                      int *map_table, int tile_idx){
    T data[...];
    int mapped_tile_idx = map_table[tile_idx];
    load_tile(data, input[mapped_tile_idx]);
    output[tile_idx] = element_wise_op(data);
}

```

Figure 6: Reordering fusion into element-wise kernel.

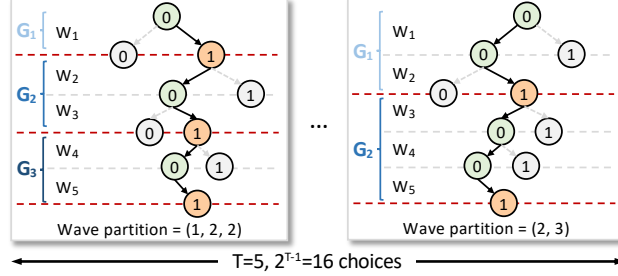


Figure 7: Design space of wave partition to form groups.

4 Real-Time Tuning

4.1 Predictive Search

We introduce a predictive search method for the tunable wave partition design in *FlashOverlap*. The proposed method first has the design space reduced from 2^{T-1} (T is the total wave number) to $\mathcal{O}(2^{T-2})$, and introduces a latency predictor to replace the online profiling. The two techniques enable the predictive search method to generate the optimized wave partition result in real time.

4.1.1 Motivation: Tuning is Necessary.

Tuning the wave partition is essential for *FlashOverlap*'s performance. We take a group containing only a wave as the baseline partition. Theoretically, the baseline partition achieves the most fine-grained overlapping. However, we conduct experiments and discover that it fails to deliver the optimal performance in most cases. Specifically, among over 50 GEMM shapes tested with the AllReduce primitive on four RTX 4090 GPUs, only 4% point to the baseline partition under exhaustive search. Employing the baseline partition leads to an average of 17.34% performance degradation. Fundamentally, such degradation results from the under-utilized bandwidth due to segmented communication, and the overhead caused by frequent API calls, which collectively become the performance bottleneck when communication latency dominates the execution.

4.1.2 Challenge: Significant Tuning Overhead.

The original tuning design space is of size 2^{T-1} , with each partition candidate requiring an online execution to select the optimal, thus leading to non-negligible tuning overhead. When dealing with varying workloads, such as serving large language models, generating pre-tuned parameters for all workloads in advance is challenging, thus necessitating real-time parameter tuning [45]. A typical GEMM output size is $M = 4096, N = 8192, K = 7168$ in computing generative models, leading to 1024 tiles with a tile size of 256×128 . An NVIDIA RTX 4090 GPU has 128 SMs, and deploying such a GEMM workload generates 8 waves ($T=8$), equaling a design space of 128 candidates. The online execution takes approximately 5ms, and the profiling tends to include 10 warm-up tests and 100 timing tests to mitigate the measurement fluctuations. Therefore, the online profiling takes more than 1 minute ($>100\times$ of model forwarding latency), which is unacceptable for end-to-end performance.

4.1.3 Insight: Overlapped Latency Decomposition.

The design space can be reduced based on prior knowledge, and the online profiling can be replaced by a cost model that predicts the latency. Considering the composition of the latency after overlapping, the overlapped computation and communication occupy the middle part of the timeline, and hence the head and tail parts of the timeline are influential. The head and the tail are determined by the first and the last group sizes, respectively. Thus, both the first and the last

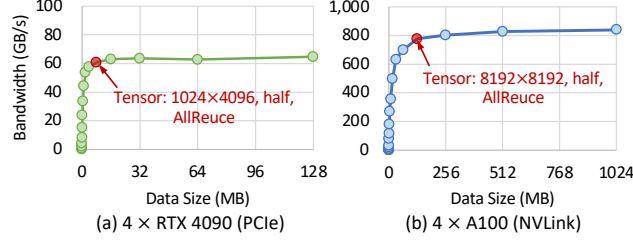


Figure 8: Inter-GPU bandwidth curve varying with data size. The red spots show borderline examples facing bandwidth degradation.

group sizes are preferred not to be too large, to avoid the cold start and the long tail. The design space can be reduced by using such a principle.

Furthermore, instead of online profiling, we can design an accurate latency prediction method as the cost model for the searching process. To achieve high prediction accuracy, the separate latency of each operation after overlapping needs analysis. (1) GEMM computation: since the main loop in GEMM is well preserved, the latency is mainly affected by the computational resource contention. (2) Communication primitive: the influential factor is the communication segmentation, leading to a prolonged latency. Based on that, the wave partition further decides the overlapping pattern.

4.1.4 Approach: Design Space Pruning and Predictive Search.

The proposed search method constrains the sizes of the first and last groups to prune the design space, and applies a latency predictor in the searching process. Specifically, we set $|G_1| \leq S_1$ and $|G_P| \leq S_P$, and use $S_1 = 2$ and $S_P = 4$ for evaluation.

Since *FlashOverlap* sets the higher priority for the communication kernel, once the SM number occupied by the communication primitive is determined, the remaining SMs are the SMs available for the GEMM computation. Considering that the utilized SMs become fewer, the latency of GEMM computation after overlapping is derived by adjusting the original latency according to the updated wave number. *FlashOverlap* estimates the communication latency based on the bandwidth curve that varies with the data amount. Specifically, the communication latency of each group is predicted with the data amount as the input, and the total communication latency is the sum of all. The detailed predicting method is illustrated in Alg. 1.

4.2 Tuning Algorithm

As shown in Alg. 1, the tuning algorithm in *FlashOverlap* is decomposed into the offline stage and the online stage. The offline stage is responsible for deriving the GEMM configuration, the communication bandwidth curve, and figuring out the resource contention on SMs. At the online stage, we build the design space and search for the optimal partition based on latency prediction.

4.2.1 Offline Stage

(1) Computation efficiency: given a problem size $M \times N \times K$, GEMM configurations are typically available, leveraging existing highly optimized linear algebra implementations (e.g., cuBLAS [46] and CUTLASS [29] on NVIDIA GPUs). The required GEMM configurations include tiling size, sizzling pattern, and the corresponding duration, etc. (2) Communication efficiency: performing a communication primitive on given GPUs, the bandwidth exhibits continuous variation with the data size, as shown in Fig. 8. Therefore, the bandwidth curve is sampled with multiple dense points, given a data size, and the effective bandwidth can be accurately estimated through interpolation of sampled points. (3) Resource contention: a communication primitive across given GPUs occupies a constant SM number using NCCL [1]. Thus, the total wave number of the GEMM computation is updated according to line 3 in Alg. 1.

4.2.2 Online Stage

(1) Generate the candidates (line 7): The original design space is the binary decision at each wave, forming a space size of 2^{T-1} . *FlashOverlap* reduces the design space with prior knowledge by constraining group size, as mentioned in Sec. 4.1. The candidate partitions are stored in *candidates*. (2) Predictive search (lines 8-26): all candidate partitions are compared based on their predicted latencies. The predicted latency is accumulated by looping over the groups in the corresponding partition. Specifically, we interpolate the current group’s communication latency (*comm_dur*), and

Algorithm 1 Grouping tuning algorithm**Input:** M, N, K # GEMM shape, $comm_op$ # communication primitive, gpu # GPU hardware

```

1: # Offline: get GEMM configuration
2:  $gemm\_config \leftarrow get\_config(M, N, K, gpu)$ 
3:  $total\_wave\_num \leftarrow gemm\_config.tile\_num / (gpu.sm\_num - comm\_op.sm\_num)$ 
4: # Offline: get the (data size, bandwidth) curve
5:  $bandwidth\_curve \leftarrow sample\_bandwidth(comm\_op, gpu)$ 
6: # Online: tuning grouping configuration
7:  $candidates \leftarrow get\_candidates(gemm\_config.wave\_num)$ 
8:  $min\_latency \leftarrow 0$ 
9: for  $group\_list$  in  $candidates$  do
10:    $acc\_comp\_dur \leftarrow 0, acc\_comm\_dur \leftarrow 0$ 
11:   for  $group$  in  $group\_list$  do
12:     # Interpolate the comm. latency of last group
13:      $data\_size \leftarrow get\_last\_group\_size(group\_list)$ 
14:      $comm\_dur \leftarrow interpolate\_latency(bandwidth\_curve, data\_size)$ 
15:     # Calculate computation latency of this group
16:      $comp\_dur \leftarrow gemm\_config.duration / total\_wave\_num \times group.wave\_num$ 
17:     # Latency accumulation
18:      $acc\_comm\_dur \leftarrow \max(acc\_comp\_dur, acc\_comm\_dur) + comm\_dur$ 
19:      $acc\_comp\_dur \leftarrow acc\_comp\_dur + comp\_dur$ 
20:   end for
21:   # Add the communication latency of the final group
22:    $data\_size \leftarrow get\_last\_group\_size(group\_list)$ 
23:    $acc\_comm\_dur \leftarrow \max(acc\_comp\_dur, acc\_comm\_dur) + interpolate\_latency(bandwidth\_curve, data\_size)$ 
24:   # Get the optimal wave partition
25:   if  $acc\_comm\_dur < min\_latency$  then
26:      $min\_latency \leftarrow acc\_comm\_dur$ 
27:      $optimal\_partition \leftarrow group\_list$ 
28:   end if
29: end for
30: return  $optimal\_partition$ 

```

derive the current group’s computation latency ($comp_dur$) based on its wave number. Based on that, the proposed algorithm accumulates the communication and computation latencies separately. Note that the GEMM computation executes without interruption, and the accumulated computation latency (acc_comp_dur) is accumulated by each group’s $comp_dur$. On the other hand, the accumulated communication latency (acc_comm_dur) is accumulated by the maximum of acc_comp_dur and acc_comm_dur , ensuring that the computation of the last wave is finished.

5 Implementation

We implement *FlashOverlap* based on the GEMM from CUTLASS [29]. The main loop of GEMM is well preserved, and we apply the optimal GEMM configuration tuned by the CUTLASS profiler. Following EVT [31], the mapping method in *FlashOverlap* is integrated into the epilogue of the GEMM, thereby avoiding the performance degradation of the main loop. The signaling mechanism is implemented using a GPU kernel, periodically querying the counting table to check the timing for triggering communication. The communication is simply achieved by calling NCCL [1] APIs. On top of the computation and the communication, *FlashOverlap* utilizes the CUDA stream [47] API to manage the concurrent execution. Specifically, the GEMM kernel is executed in a stream, while the signaling kernels and the communication kernels are executed in another stream. For each group, the signaling kernel stalls the communication until the number in the counting table meets the corresponding group size.

6 Evaluation

We evaluate the operator-level performance of *FlashOverlap* with various communication primitives on different types of GPUs. *FlashOverlap* delivers 69-98% of the theoretical performance and achieves an average of $1.07\text{-}1.31 \times$

Table 3: GEMM shapes in operator evaluation (on each GPU).

Primitive	AllReduce		ReduceScatter		All-to-All
	A800	4090	A800	4090	A800
$M \times N (\times 1024^2)$	64~256	16~64	64~256	16~64	8~48
$K (\times 1024)$	4~8	8~16	4~8	8~16	4~8

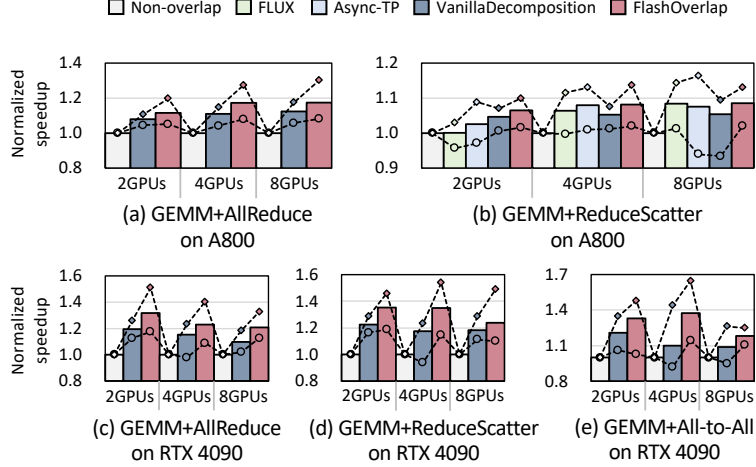


Figure 9: Operator-level speedup comparison, higher is better. "○" and "◇" denote the minimum and maximum normalized speedups, respectively.

speedups with various primitives, outperforming other baselines in most cases. Furthermore, we conduct experiments to demonstrate the effectiveness of the proposed predictive searching method and quantify the overhead of reordering.

6.1 Setup

6.1.1 Testbed

We conduct experiments on both NVIDIA A800 GPUs and RTX 4090 GPUs. The server with A800 GPUs equips pairwise NVLink [14] connecting each of the two GPUs, while the server with RTX 4090 GPUs builds the inter-GPU connection traversing PCIe [32] across NUMA [48] nodes. The corresponding inter-GPU bandwidths are illustrated in Fig. 8. The corresponding software environment includes CUDA 12.2 [49], NCCL 2.19.3 [1], PyTorch 2.5.1 [50], and CUTLASS 3.4.0 [29].

6.1.2 Benchmark

We benchmark the latency of GEMM+AllReduce, GEMM+ReduceScatter, and GEMM+All-to-All, tested under different parallelism settings and over 200 GEMM sizes from real-world workloads. The detailed sizes are presented in Tab. 3.

6.1.3 Baseline

We use both decomposition-based and fusion-based methods as baselines. One of the decomposition-based baselines is Async-TP [40] by PyTorch [50]. Since Async-TP requires an NVLink connection between all GPU pairs, we further develop another decomposition-based baseline utilizing cuBLAS [46] and NCCL [1] APIs (denoted as VanillaDecomposition). We use FLUX [21] as the baseline for the fusion-based method. FLUX requires peer-to-peer access, which the tested RTX 4090 server does not support. The non-overlap baseline is the implementation of the sequential execution of GEMM and communication based on cuBLAS and NCCL APIs, respectively.

6.2 Operator-Level Performance

The operator-level evaluation compares the total latency of the computation and the communication. We collect the latency and calculate the speedup of each implementation normalized to the non-overlap baseline. As shown in Fig. 9, the speedup is the average number across multiple GEMM sizes within the corresponding range in Table 3.

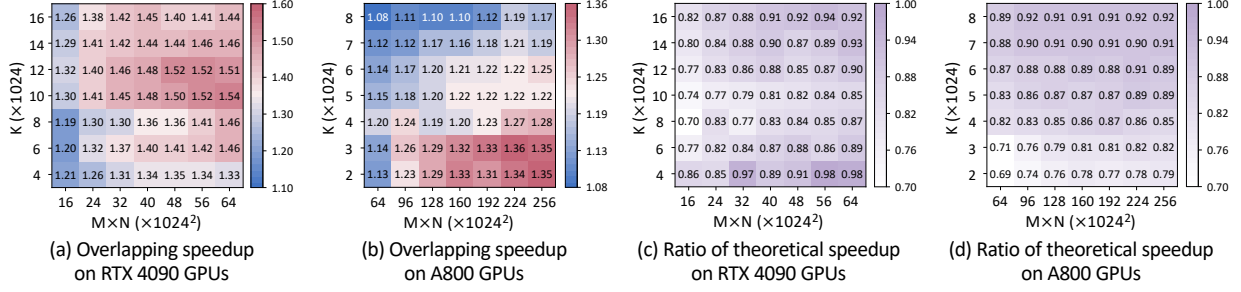
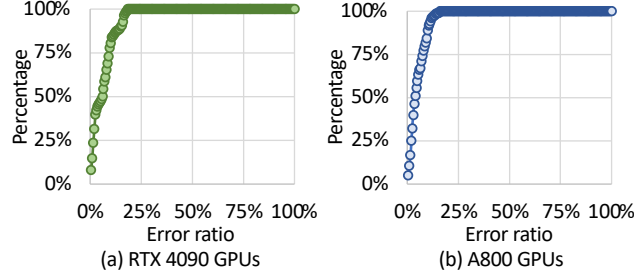
Figure 10: Heatmap of *FlashOverlap* performance across different GEMM sizes.

Figure 11: Cumulative distribution function of prediction error ratio.

Most baselines support GEMM+ReduceScatter on GPUs with peer-to-peer access, as shown in Fig. 9(b). Compared to baselines, *FlashOverlap* achieves higher average speedup across all cases, and effectively avoids performance deterioration, benefiting from interference-free computation and highly predictable overlapping performance. Given that NVLink decreases communication time proportion, *FlashOverlap* delivers less speedup on A800 GPUs compared to RTX 4090 GPUs. However, the achieved speedup ratio of *FlashOverlap* on the A800 GPUs relative to its theoretical speedup demonstrates a competitive result, as evidenced in Fig. 10(d). On RTX 4090 GPUs, *FlashOverlap* achieves $1.02\text{-}1.65\times$ speedup over the non-overlap baseline, and $0.93\text{-}1.46\times$ speedup over the decomposition-based method.

6.3 Theoretical Analysis

The speedups of *FlashOverlap* across different GEMM sizes are depicted in Fig. 10 (a) and (b). The data on RTX 4090 GPUs and A800 GPUs are collected with ReduceScatter (TP=2) and AllReduce (TP=4), respectively. In the figure, the number along x -axis is the product of M and N ($M \times N$), which determines the total communication data size, while the number along y -axis is the size of K that controls the ratio between computation workload and communication data size, *i.e.*, the ratio between computation and communication latencies. The speedup exhibits significant variations across different GEMM sizes, and displays different patterns on different GPUs. We observe that *FlashOverlap* performs better within a specific $M \times N \times K$ region, where the computation and communication latencies are close and lead to better overlapping opportunity. Such a region is influenced by both GPU computational capability and inter-GPU bandwidth. Specifically, on A800 GPUs, due to the high bandwidth of NVLink, the speedup is higher with smaller K , where the reduced computation workload better balances with the shortened communication latency.

To further understand the performance of *FlashOverlap*, we compare the speedup to a theoretical upper bound. Assuming the overlapping is perfect, the theoretical latency is calculated by summing up the original GEMM latency and the communication latency of the final wave (if GEMM takes more time), or the GEMM latency of the first wave and the original communication latency (if communication takes more time). *FlashOverlap* achieves over 80% of the theoretical speedup in most cases. The ratio falls below 1 because of (1) segmented communication leading to under-utilized bandwidth and (2) the prolonged computation latency brought by SM contention. Therefore, the ratio is suboptimal on both GPUs with smaller $M \times N$, as a small data amount, especially when segmented, fails to effectively utilize the bandwidth.

6.4 Searching Method Evaluation

The proposed predictive search depends on a predictor to reduce the online profiling overhead, and we measure the prediction error ratios under more than 250 combinations of different sizes, grouping partitions, and parallelism settings

Table 4: Latency increase brought by the fusion of remapping in an RMSNorm GPU kernel.

	A800 GPU			RTX 4090 GPU		
	Tile	Subtile	Token	Tile	Subtile	Token
Ratio	9.27%	12.6%	13.4%	5.76%	3.43%	7.07%

on each type of GPU. The cumulative distribution function (CDF) of the prediction error ratio is depicted in Fig. 11, and the average error ratios are 3.41% and 3.44% on RTX 4090 GPUs and A800 GPUs, respectively. Due to non-ideal implementation, the actual latency is always slightly higher than the predicted latency, but both demonstrate similar trends across different partitions, enabling the searched partition to be nearly optimal. To demonstrate that, we compare the performance between the searched partition and the optimal partition. Based on such a high-accuracy predictor, the searched partition achieves $> 99\%$ performance of the optimal one. Therefore, we directly apply the prediction-based searching in all the evaluation experiments.

6.5 Overhead Analysis

To measure the overhead brought by reordering, we implement an RMSNorm GPU kernel fused with the remapping operation. As mentioned in Sec. 3.3, the mapping and remapping operations can have various types of granularity, and the implemented RMSNorm kernel supports all of the tile-level, subtile-level, and token-level remapping. As shown in Tab. 4, the fusion of the remapping operation brings about 3%~13% extra latency in RMSNorm. The token-level remapping brings a relatively higher increase due to more irregular memory access, which is still inherently marginal considering the negligible latency of the element-wise operator. Since remapping is the reverse operation of mapping, it is feasible to remove the mapping overhead via the fusion to the GEMM epilogue. The mapping overhead has already been counted into the operator latency.

7 Conclusion

In this paper, we introduce *FlashOverlap*, a signaling-based lightweight overlapping design. *FlashOverlap* utilizes the signals to trigger communication, while preserving the computation process. Based on the signaling mechanism, we demonstrate that the tile-wise signaling can be resolved into waves to mitigate communication fragmentation. Besides, we employ a pair of pre-communication and post-communication reordering operations to ensure communication continuity, and the overhead of both is optimized via kernel fusion. Furthermore, we enable the design of *FlashOverlap* to be tunable via wave grouping, and propose a predictive search method to optimize the wave group size selection. Experiments show that *FlashOverlap* achieves an average of $1.07\text{--}1.31\times$ speedups with various primitives.

References

- [1] NVIDIA. Nvidia collective communication library. [Online], 2025. <https://docs.nvidia.com/deeplearning/ncc1>.
- [2] DeepSeek-AI. Deepseek-v3 technical report. *arXiv preprint arXiv:2412.19437v1*, 2024.
- [3] Llama3 Team. The llama 3 herd of models. 2024.
- [4] OpenAI. Chatgpt. [Online], 2025. <https://chatgpt.com/>.
- [5] Mark Chen, Jerry Tworek, Heewoo Jun, Qiming Yuan, Henrique Ponde de Oliveira Pinto, Jared Kaplan, Harri Edwards, Yuri Burda, Nicholas Joseph, Greg Brockman, et al. Evaluating large language models trained on code. *arXiv preprint arXiv:2107.03374*, 2021.
- [6] Baptiste Rozière, Jonas Gehring, Fabian Gloeckle, Sten Sootla, Itai Gat, Xiaoqing Ellen Tan, Yossi Adi, Jingyu Liu, Romain Sauvestre, Tal Remez, Jérémy Rapin, Artyom Kozhevnikov, Ivan Evtimov, Joanna Bitton, Manish Bhatt, Cristian Canton Ferrer, Aaron Grattafiori, Wenhan Xiong, Alexandre Défossez, Jade Copet, Faisal Azhar, Hugo Touvron, Louis Martin, Nicolas Usunier, Thomas Scialom, and Gabriel Synnaeve. Code llama: Open foundation models for code. *arXiv preprint arXiv:2308.12950*, 2023.
- [7] Uriel Singer, Adam Polyak, Thomas Hayes, Xi Yin, Jie An, Songyang Zhang, Qiyuan Hu, Harry Yang, Oron Ashual, Oran Gafni, Devi Parikh, Sonal Gupta, and Yaniv Taigman. Make a video: Text-to-video generation without text-video data. *arXiv preprint arXiv:2209.14792*, 2022.
- [8] Wenyi Hong, Ming Ding, Wendi Zheng, Xinghan Liu, and Jie Tang. Cogvideo: Large-scale pretraining for text-to-video generation via transformers. *arXiv preprint arXiv:2205.15868*, 2022.

- [9] Zhuoyi Yang, Jiayan Teng, Wendi Zheng, Ming Ding, Shiyu Huang, Jiazheng Xu, Yuanming Yang, Wenyi Hong, Xiaohan Zhang, Guanyu Feng, et al. Cogvideox: Text-to-video diffusion models with an expert transformer. *arXiv preprint arXiv:2408.06072*, 2024.
- [10] Alibaba Group Wan Team. Wan: Open and advanced large-scale video generative models. *arXiv preprint arXiv:2503.20314*, 2025.
- [11] Zijun Liu, Yanzhe Zhang, Peng Li, Yang Liu, and Diyi Yang. Dynamic llm-agent network: An llm-agent collaboration framework with agent team optimization, 2023.
- [12] Xu Huang, Weiwen Liu, Xiaolong Chen, Xingmei Wang, Hao Wang, Defu Lian, Yasheng Wang, Ruiming Tang, and Enhong Chen. Understanding the planning of llm agents: A survey. *arXiv preprint arXiv:2402.02716*, 2024.
- [13] Meta. The llama 4 herd: The beginning of a new era of natively multimodal ai innovation. [Online], 2025. <https://ai.meta.com/blog/llama-4-multimodal-intelligence/>.
- [14] NVIDIA. The building blocks of high-speed, multi-gpu communication for feeding large datasets faster into models and rapidly exchanging data between gpus. [Online], 2025. <https://www.nvidia.com/en-us/data-center/nvlink/>.
- [15] Abhinav Jangda, Jun Huang, Guodong Liu, Amir Hossein Nodehi Sabet, Saeed Maleki, Youshan Miao, Madanlal Musuvathi, Todd Mytkowicz, and Olli Saarikivi. Breaking the computation and communication abstraction barrier in distributed machine learning workloads. In *Proceedings of the 27th ACM International Conference on Architectural Support for Programming Languages and Operating Systems*, 2022.
- [16] Guanhua Wang, Chengming Zhang, Zheyu Shen, Ang Li, and Olatunji Ruwase. Domino: Eliminating communication in llm training via generic tensor slicing and overlapping. *arXiv preprint arXiv:2409.15241*, 2024.
- [17] Shibo Wang, Jinliang Wei, Amit Sabne, Andy Davis, Berkin Ilbeyi, Blake Hechtman, Dehao Chen, Karthik Srinivasa Murthy, Marcello Maggioni, Qiao Zhang, Sameer Kumar, Tongfei Guo, Yuanzhong Xu, and Zongwei Zhou. Overlap communication with dependent computation via decomposition in large deep learning models. In *Proceedings of the 28th ACM International Conference on Architectural Support for Programming Languages and Operating Systems*, 2023.
- [18] Chang Chen, Xiuhong Li, Qianchao Zhu, Jiangfei Duan, Peng Sun, Xingcheng Zhang, and Chao Yang. Centauri: Enabling efficient scheduling for communication-computation overlap in large model training via communication partitioning. In *Proceedings of the 29th ACM International Conference on Architectural Support for Programming Languages and Operating Systems*, pages 178–191, 2024.
- [19] DeepSeek-AI. DeepEP: an efficient expert-parallel communication library, 2025. <https://github.com/deepseek-ai/DeepEP>.
- [20] Ziheng Jiang, Haibin Lin, Yinmin Zhong, Qi Huang, Yangrui Chen, Zhi Zhang, Yanghua Peng, Xiang Li, Cong Xie, Shibiao Nong, Yulu Jia, Sun He, Hongmin Chen, Zhihao Bai, Qi Hou, Shipeng Yan, Ding Zhou, Yiyao Sheng, Zhuo Jiang, Haohan Xu, Haoran Wei, Zhang Zhang, Pengfei Nie, Leqi Zou, Sida Zhao, Liang Xiang, Zherui Liu, Zhe Li, Xiaoying Jia, Jianxi Ye, Xin Jin, and Xin Liu. Overlap communication with dependent computation via decomposition in large deep learning models. In *Proceedings of the 21st USENIX Symposium on Networked System Design and Implementation*, 2024.
- [21] Li-Wen Chang, Wenlei Bao, Qi Hou, Chengquan Jiang, Ningxin Zheng, Yinmin Zhong, Xuanrun Zhang, Zuquan Song, Ziheng Jiang, Haibin Lin, Xin Jin, and Xin Liu. Flux: Fast software-based communication overlap on gpus through kernel fusion. *arXiv preprint arXiv:2406.06858*, 2024.
- [22] Kishore Punniyamurthy, Khaled Hamidouche, and Bradford M. Beckmann. Optimizing distributed ml communication with fused computation-collective operations. In *Proceedings of the International Conference for High Performance Computing, Networking, Storage, and Analysis*, pages 1–17, 2024.
- [23] Shulai Zhang, Ningxin Zheng, Haibin Lin, Ziheng Jiang, Wenlei Bao, Chengquan Jiang, Qi Hou, Weihao Cui, Size Zheng, Li-Wen Chang, Quan Chen, and Xin Liu. Comet: Fine-grained computation-communication overlapping for mixture-of-experts. In *Proceedings of the 8th Annual Conference on Machine Learning and Systems*, 2025.
- [24] Hulin Wang, Yaqi Xia, Donglin Yang, Xiaobo Zhou, and Dazhao Cheng. Harnessing inter-gpu shared memory for seamless moe communication-computation fusion. In *Proceedings of the 30th ACM SIGPLAN Annual Symposium on Principles and Practice of Parallel Programming*, 2025.
- [25] NVIDIA. cublasmp: A high-performance cuda library for distributed dense linear algebra, 2025. <https://docs.nvidia.com/cuda/cublasmp/>.
- [26] Size Zheng, Jin Fang, Xuegui Zheng, Qi Hou, Wenlei Bao, Ningxin Zheng, Ziheng Jiang, Dongyang Wang, Jianxi Ye, Haibin Lin, Li-Wen Chang, and Xin Liu. Tilelink: Generating efficient compute-communication overlapping kernels using tile-centric primitives. *arXiv preprint arXiv:2503.20313*, 2025.

- [27] NVIDIA. Parallel thread execution isa version 8.7. [Online], Feb 2025. <https://docs.nvidia.com/cuda/parallel-thread-execution>.
- [28] NVIDIA. Gpu performance background user’s guide. [Online], Feb 2023. <https://docs.nvidia.com/deeplearning/performance/dl-performance-gpu-background>.
- [29] NVIDIA. Cutlass: Cuda templates for linear algebra subroutines. [Online], 2017. <https://github.com/NVIDIA/cutlass>.
- [30] Muhammad Osama, Duane Merrill, Cris Cecka, Michael Garland, and John D. Owens. Stream-k: Work-centric parallel decomposition for dense matrix-matrix multiplication on the gpu. pages 429–431, 2023.
- [31] Zhaodong Chen, Andrew Kerr, Richard Cai, Jack Kosaian, Haicheng Wu, Yufei Ding, and Yuan Xie. Evt: Accelerating deep learning training with epilogue visitor tree. In *Proceedings of the 29th ACM SIGPLAN Annual Symposium on Principles and Practice of Parallel Programming*, 2024.
- [32] PCI-SIG. Pci express 6.0 specification. [Online], 2025. <https://pcisig.com/pci-express-6.0-specification>.
- [33] NVIDIA. Infiniband. [Online], 2025. <https://www.nvidia.com/en-us/networking/products/infiniband/>.
- [34] Pitch Patarasuk and Xin Yuan. Bandwidth optimal all-reduce algorithms for clusters of workstations. *Journal of Parallel and Distributed Computing*, 9:117–124, 2009.
- [35] Meghan Cowan, Saeed Maleki, Madanlal Musuvathi, Olli Saarikivi, and Yifan Xiong. Mscclang: Microsoft collective communication language. In *Proceedings of the 28th ACM International Conference on Architectural Support for Programming Languages and Operating Systems, Volume 2*, pages 502–514, 2023.
- [36] Mohammad Shoeybi, Mostofa Patwary, Raul Puri, Patrick LeGresley, Jared Casper, and Bryan Catanzaro. Megatron-lm: Training multi-billion parameter language models using model parallelism. *arXiv preprint arXiv:1909.08053*, 2019.
- [37] Shen Li, Yanli Zhao, Rohan Varma, Omkar Salpekar, Pieter Noordhuis, Teng Li, Adam Paszke, Jeff Smith, Brian Vaughan, Pritam Damania, and Soumith Chintala. Pytorch distributed: Experiences on accelerating data parallel training. *arXiv preprint arXiv:2006.15704*, 2020.
- [38] Yanli Zhao, Andrew Gu, Rohan Varma, Liang Luo, Chien-Chin Huang, Min Xu, Less Wright, Hamid Shojanazeri, Myle Ott, Sam Shleifer, Alban Desmaison, Can Balioglu, Pritam Damania, Bernard Nguyen, Geeta Chauhan, Yuchen Hao, Ajit Mathews, and Shen Li. Pytorch fsdp: Experiences on scaling fully sharded data parallel. In *Proceedings of the VLDB Endowment*, pages 3848–3860, 2023.
- [39] Dmitry Lepikhin, HyukJoong Lee, Yuanzhong Xu, Dehao Chen, Orhan Firat, Yanping Huang, Maxim Krikun, Noam Shazeer, and Zhifeng Chen. Gshard: Scaling giant models with conditional computation and automatic sharding. In *International Conference on Learning Representations*, 2021.
- [40] PyTorch. Introducing async tensor parallelism in pytorch. [Online], Sep 2024. <https://discuss.pytorch.org/t/distributed-w-torchtitan-introducing-async-tensor-parallelism-in-pytorch/209487>.
- [41] Suchita Pati, Shaizeen Aga, Mahzabeen Islam, Nuwan Jayasena, and Matthew D Sinclair. T3: Transparent tracking & triggering for fine-grained overlap of compute & collectives. In *Proceedings of the 29th ACM International Conference on Architectural Support for Programming Languages and Operating Systems, Volume 2*, pages 1146–1164, 2024.
- [42] Haiquan Wang, Chaoyi Ruan, Jia He, Jiaqi Ruan, Chengjie Tang, Xiaosong Ma, and Cheng Li. Hiding communication cost in distributed llm training via micro-batch co-execution. *arXiv preprint arXiv:2411.15871*, 2024.
- [43] Chenyu Jiang, Ye Tian, Zhen Jia, Shuai Zheng, Chuan Wu, and Yida Wang. Lancet: Accelerating mixture-of-experts training via whole graph computation-communication overlapping. In *Proceedings of the 7th Annual Conference on Machine Learning and Systems*, 2024.
- [44] Jiaao He, Jidong Zhai, Tiago Antunes, Haojie Wang, Fuwen Luo, Shangfeng Shi, and Qin Li. Fastermoe: modeling and optimizing training of large-scale dynamic pre-trained models. In *Proceedings of the 27th ACM SIGPLAN Symposium on Principles and Practice of Parallel Programming*, 2022.
- [45] Ke Hong, Guohao Dai, Jiaming Xu, Qiuli Mao, Xiuhong Li, Jun Liu, Kangdi Chen, Yuhang Dong, and Yu Wang. Flashdecoding++: Faster large language model inference with asynchronization, flat gemm optimization, and heuristics. In *Proceedings of the 7th Annual Conference on Machine Learning and Systems*, 2024.

- [46] NVIDIA. cublas: Basic linear algebra on nvidia gpus. [Online], 2017. <https://developer.nvidia.com/cublas>.
- [47] NVIDIA. Stream management functions of the low-level cuda driver application programming interface. [Online], 2025. <https://docs.nvidia.com/cuda/cuda-driver-api/>.
- [48] Christoph Lameter. Numa (non-uniform memory access): An overview. *Queue*, 11(7):40–51, July 2013.
- [49] Nvidia. Cuda toolkit. [Online], June 2025. <https://developer.nvidia.com/cuda-toolkit>.
- [50] Adam Paszke, Sam Gross, Francisco Massa, Adam Lerer, James Bradbury, Gregory Chanan, Trevor Killeen, Zeming Lin, Natalia Gimelshein, Luca Antiga, Alban Desmaison, Andreas Kopf, Edward Yang, Zachary DeVito, Martin Raison, Alykhan Tejani, Sasank Chilamkurthy, Benoit Steiner, Lu Fang, Junjie Bai, and Soumith Chintala. Pytorch: An imperative style, high-performance deep learning library. *Advances in neural information processing systems*, 32, 2019.